JOC Article

New Cruciform Structures: Toward Coordination Induced Single Molecule Switches

Sergio Grunder,[†] Roman Huber,[§] Viviana Horhoiu,[†] Maria Teresa González,[§] Christian Schönenberger,[§] Michel Calame,*[,§] and Marcel Mayor*[,†,‡]

Department of Chemistry, University of Basel, St. Johanns-Ring 19, 4056 Basel, Switzerland, Institute for Physics, Klingelbergstrasse 82, University of Basel, 4056 Basel, Switzerland, and Institute for Nanotechnology, Forschungszentrum Karlsruhe GmbH, P.O. Box 3640, 76021 Karlsruhe, Germany

marcel.mayor@unibas.ch; michel.calame@unibas.ch

Received June 27, 2007

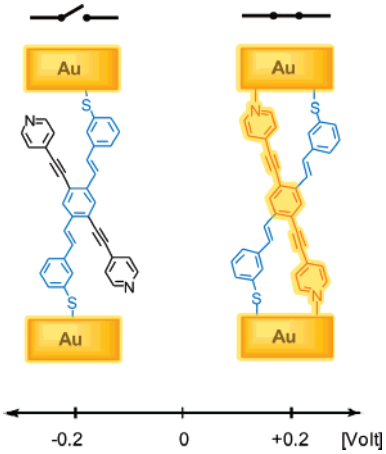

New cruciform structures **1**−**4** were synthesized to investigate a new single molecule switching mechanism arising from the interplay between the molecule and the electrode surface. These molecular cruxes consist of two rod-type substructures, namely an oligophenylenevinylene and an oligophenyleneethynyl. While the oligophenylenevinylene rods are functionalized with acetyl protected sulfur anchor groups, the oligophenyleneethynyl rods provide terminal pyridine units. The hypothesized switching mechanism should arise from the electrochemical potential dependent coordination of the pyridine unit to the electrode surface. The assembly of the oligophenylenevinylene substructure was based on a Wittig reaction whereas its perpendicular oligophenyleneethynyl rod was assembled by Sonogashira−Hagihara coupling reactions. Preliminary transport investigations with molecular cruciforms **2** and **4** in a mechanical controllable break junction in a liquid environment displayed the trapping of single molecules between two gold electrodes via the terminally sulfur functionalized oligophenylenevinylene rod.

Introduction

The semiconductor industry has seen a remarkable miniaturization trend of silicon-based integrated circuits during the past four decades. However, further decrease in feature size becomes increasingly difficult due to both physical and economical limitations.[1,2] The currently growing interest in alternative concepts to further reduce the feature size at reasonable prices is not surprising and led to a revival of molecular electronics,[1−7] a concept originating in the seventies.[8,9] In the

* Address correspondence concerning chemical synthesis, experimental and molecular design to Marcel Mayor. Phone: +41-61-267-1006. Fax: +41-61-267-1016. Address correspondence concerning break junction investigations to Michel Calame. Phone: +41-61-267-3697. Fax: +41-61-267-3784.
[†] Department of Chemistry, University of Basel.
[§] Institute for Physics, University of Basel.
[‡] Institute for Nanotechnology, Forschungszentrum Karlsruhe GmbH.

(1) Joachim, C.; Gimzewski, J. K.; Aviram, A. *Nature* (*London*) **2000**, *408*, 541−548.
(2) Mayor, M.; Weber, H. B. *Chimia* **2003**, *56*, 494−499.
(3) Weibel, N.; Grunder, S.; Mayor, M. *Org. Biomol. Chem.* **2007**, *5*, 2343−2353.
(4) Tao, N. J. *Nat. Nanotechnol.* **2006**, *1*, 173−181.

10.1021/jo7013998 CCC: $37.00
Published on Web 10/04/2007

past few years, numerous molecular structures have been integrated as small assemblies or even on a single molecule level in various setups to investigate both their structure property correlations and their potential as the origin of the electronic function.[2,10−12] Recently, even electronic functions like, e.g., rectification[13,14] or hysteretic switching[15,16] emerging from integrated molecules have been reported. However, to trace the origin of the observed electronic features remains very challenging. To differentiate between effects arising from the molecular structure or from the molecule electrode interface is exceedingly delicate,[10,17] in particular on a single molecule level. Therefore, current comprehensive models consider both the molecular structure and the contact area of the electrodes.[6]

Here we would like to propose a new switching concept for integrated molecules emerging from the interplay between the molecular structure and the electrode surface. So far, several concepts for molecular switches have already been proposed and some of them have already been realized for derivatives integrated in an electronic circuit. Light triggered photoreactions[18] and electrochemically active chromophores[19−22] have been used or proposed to alter the conjugation along a molecular structure. Electrochemical charging of subunits altered transport properties through an integrated redox active subunit[23] and has been successfully applied to rearrange mechanical interlinked structures in supermolecules.[24,25] Integrated molecules reacting with an analyte have been reported as switches but also as potential sensing devices.[26,27] Furthermore, there are several reported integrated molecule based devices displaying promising electronic features like hysteretic switching[15] or negative differential resistance[28] for which the origin of the observed effect is the topic of current investigations.

To the best of our knowledge, conductance switching concepts based on the interplay of the molecular structure with the electrode surface have not been proposed so far. Together with the switching concept we present the synthesis and characterization of the cruciform structures **1** and **2**. Furthermore, first attempts to integrate these molecules in a mechanically controlled break-junction (MCBJ) in a liquid environment are shown. Structurally related cruciform π-systems have already been reported as test structures for molecular electronics,[29,30] as electrooptically active chromophores in self-assembled thin films,[31,32] as chromophores with tunable band gaps,[33] as metal ion[34,35] or pH-[36]sensors,[37] and as building blocks of coordination polymers.[38]

Reversible potential dependent coordination of nitrogen-containing heterocycles to metal substrates has been observed in electrochemical scanning probe investigations.[11,39] Interestingly, upon coordination, the π-system of the heterocycle is expected to couple strongly with the electrodes fermi level. In contrast to that, the sulfur noble metal bond is known to provide a considerable tunnel barrier for electronic transport.[40,41] Furthermore, the extent of coupling of the sulfur anchor group strongly depends on the relative substitution position with respect to the molecules backbone,[42] providing further tunability of the resistivity through the integrated structure.

The here proposed switching mechanism profits from the subtle interplay between molecule and electrode (Figure 1). The two rod-like π-systems crossing each other in the target structures **1** and **2** (Figure 1) are both able to bridge the gap between the electrodes. However, they are expected to display different surface potential dependent behavior. While one of the rods bears terminal sulfur groups, the second transversal

(5) Carroll, R. L.; Gorman, C. B. *Angew. Chem., Int. Ed.* **2002**, *41*, 4378−4400.
(6) Nitzan, A.; Ratner, M. A. *Science* (*Washington, DC, U.S.*) **2003**, *300*, 1384−1389.
(7) Heath, J. R.; Ratner, M. A. *Phys. Today* **2003**, *56*, 43−49.
(8) Mann, B.; Kuhn, H. *J. Appl. Phys.* **1971**, *42*, 4398−4405.
(9) Aviram, A.; Ratner, M. A. *Chem. Phys. Lett.* **1974**, *29*, 277−283.
(10) Cui, X. D.; Primak, A.; Zarate, X.; Tomfohr, J.; Sankey, O. F.; Moore, A. L.; Moore, T. A.; Gust, D.; Harris, G.; Lindsay, S. M. *Science* (*Washington, DC, U.S.*) **2001**, *294*, 571−574.
(11) Xu, B.; Tao, N. J. *Science* (*Washington, DC, U.S.*) **2003**, *301*, 1221−1223.
(12) Selzer, Y.; Allara, D. L. *Annu. Rev. Phys. Chem.* **2006**, *57*, 593−623.
(13) Elbing, M.; Ochs, R.; Koentopp, M.; Fischer, M.; von Hänisch, C.; Weigend, F.; Evers, F.; Weber Heiko, B.; Mayor, M. *Proc. Natl. Acad. Sci. U.S.A.* **2005**, *102*, 8815−8820.
(14) Metzger, R. M. *Acc. Chem. Res.* **1999**, *32*, 950−957.
(15) Lörtscher, E.; Ciszek, J. W.; Tour, J.; Riel, H. *Small* **2006**, *2*, 973−977.
(16) Luo, Y.; Collier, C. P.; Jeppesen, J. O.; Nielsen, K. A.; Delonno, E.; Ho, G.; Perkins, J.; Tseng, H.-R.; Yamamoto, T.; Stoddart, J. F.; Heath, J. R. *ChemPhysChem* **2002**, *3*, 519−525.
(17) Zhirnov, V. V.; Cavin, R. K. *Nat. Mater.* **2006**, *5*, 11−12.
(18) Dulic, D.; van der Molen, S. J.; Kudernac, T.; Jonkman, H. T.; de Jong, J. J. D.; Bowden, T. N.; van Esch, J.; Feringa, B. L.; van Wees, B. J. *Phys. Rev. Lett.* **2003**, *91*, 207402/1−207402/4.
(19) Li, Z.; Han, B.; Meszaros, G.; Pobelov, I.; Wandlowski, T.; Błaszczyk, A.; Mayor, M. *Faraday Discuss.* **2006**, *131*, 121−143.
(20) Sorensen, J. K.; Vestergaard, M.; Kadziola, A.; Kils, K.; Nielsen, M. B. *Org. Lett.* **2006**, *8*, 1173−1176.
(21) Li, X.; Xu, B.; Xiao, X.; Yang, X.; Zang, L.; Tao, N. *Faraday Discuss.* **2006**, *131*, 111−120.
(22) Xu, B. Q.; Li, X. L.; Xiao, X. Y.; Sakaguchi, H.; Tao, N. J. *Nano Lett.* **2005**, *5*, 1491−1495.
(23) van Dijk Elisabeth, H.; Myles Daniel, J. T.; van der Veen Marleen, H.; Hummelen Jan, C. *Org. Lett.* **2006**, *8*, 2333−2336.
(24) Steuerman, D. W.; Tseng, H.-R.; Peters, A. J.; Flood, A. H.; Jeppesen, J. O.; Nielsen, K. A.; Stoddart, J. F.; Health, J. R. *Angew. Chem., Int. Ed.* **2004**, *43*, 6486−6491.
(25) Choi, J. W.; Flood, A. H.; Steuerman, D. W.; Nygaard, S.; Braunschweig, A. B.; Moonen, N. N. P.; Laursen, B. W.; Luo, Y.; DeIonno, E.; Peters, A. J.; Jeppesen, J. O.; Xu, K.; Stoddart, J. F.; Heath, J. R. *Chem.−Eur. J.* **2005**, *12*, 261−279.
(26) Guo, X.; Whalley, A.; Klare, J. E.; Huang, L.; O'Brien, S.; Steigerwald, M.; Nuckolls, C. *Nano Lett.* **2007**, *7*, 1119−1122.
(27) Xiao, X.; Xu, B.; Tao, N. *Angew. Chem., Int. Ed.* **2004**, *43*, 6148−6152.
(28) Chen, J.; Wang, W.; Reed, M. A.; Rawlett, A. M.; Price, D. W.; Tour, J. M. *Appl. Phys. Lett.* **2000**, *77*, 1224−1226.
(29) Błaszczyk, A.; Fischer, M.; Von Hänisch, C.; Mayor, M. *Eur. J. Org. Chem.* **2007**, *2007*, 2630−2642.
(30) Klare, J. E.; Tulevski, G. S.; Sugo, K.; de Picciotto, A.; White, K. A.; Nuckolls, C. *J. Am. Chem. Soc.* **2003**, *125*, 6030−6031.
(31) Kang, H.; Zhu, P.; Yang, Y.; Facchetti, A.; Marks, T. J. *J. Am. Chem. Soc.* **2004**, *126*, 15974−15975.
(32) Kang, H.; Evmenenko, G.; Dutta, P.; Clays, K.; Song, K.; Marks, T. J. *J. Am. Chem. Soc.* **2006**, *128*, 6194−6205.
(33) Wilson, J. N.; Josowicz, M.; Wang, Y.; Bunz, U. H. F. *Chem. Commun.* (*Cambridge, U.K.*) **2003**, 2962−2963.
(34) Wilson, J. N.; Bunz, U. H. F. *J. Am. Chem. Soc.* **2005**, *127*, 4124−4125.
(35) Hauck, M.; Schoenhaber, J.; Zucchero, A. J.; Hardcastle, K. I.; Mueller, T. J. J.; Bunz, U. H. F. *J. Org. Chem.* **2007**, *72*, 6714−6725.
(36) McGrier, P. L.; Solntsev, K. M.; Schoenhaber, J.; Brombosz, S. M.; Tolbert, L. M.; Bunz, U. H. F. *Chem. Commun.* (*Cambridge, U.K.*) **2007**, 2127−2129.
(37) Zucchero, A. J.; Wilson, J. N.; Bunz, U. H. F. *J. Am. Chem. Soc.* **2006**, *128*, 11872−11881.
(38) Gerhardt, W. W.; Zucchero, A. J.; Wilson, J. N.; South, C. R.; Bunz, U. H. F.; Weck, M. *Chem. Commun.* (*Cambridge, U.K.*) **2006**, 2141−2143.
(39) Mayer, D.; Dretschkow, T.; Ataka, K.; Wandlowski, T. *J. Electroanal. Chem.* **2002**, *524−525*, 20−35.
(40) Hipps, K. W. *Science* (*Washington, DC, U.S.*) **2001**, *294*, 536−537.
(41) Chen, F.; Li, X.; Hihath, J.; Huang, Z.; Tao, N. *J. Am. Chem. Soc* **2006**, *128*, 15874−15881.
(42) Mayor, M.; Weber Heiko, B.; Reichert, J.; Elbing, M.; von Hänisch, C.; Beckmann, D.; Fischer, M. *Angew. Chem., Int. Ed.* **2003**, *42*, 5834−5838.

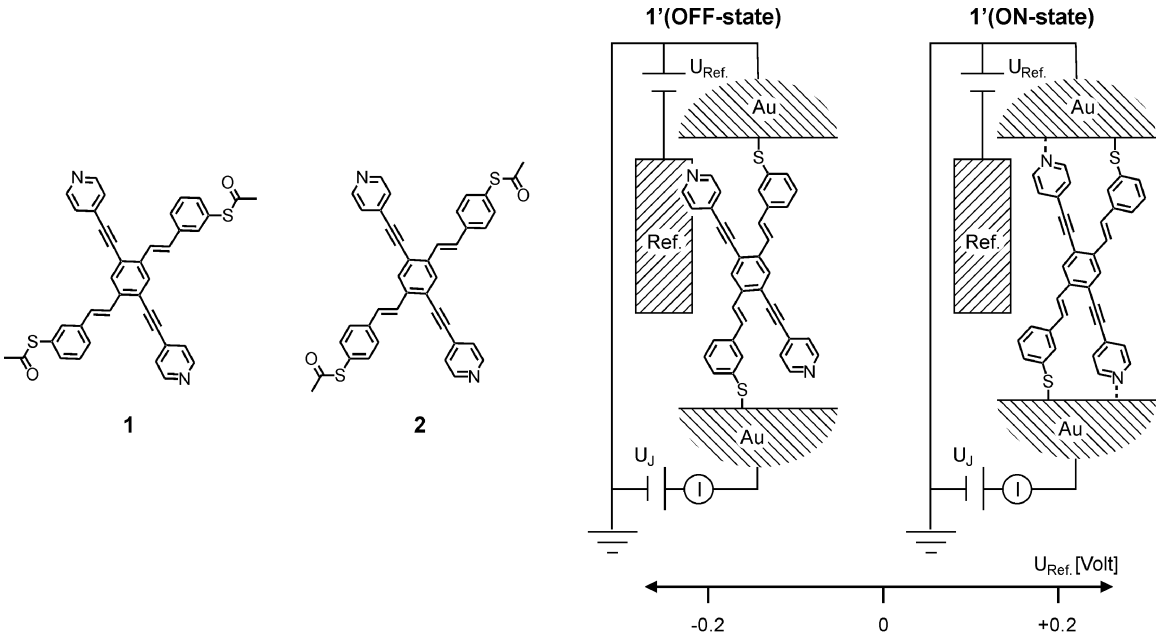

FIGURE 1. Target structures **1** and **2** and hypothesized potential dependent switching mechanism in an electrochemical setup.

rod is functionalized terminally with pyridine subunits. The task of the sulfur functionalized oligophenylenevinylene (OPV) rod is solely to fix the molecule in the junction. Even though the delocalized π-system of the OPV rod favors electronic transport, the sulfur anchor groups of **1** and **2** considerably reduce the electronic transport features through this channel. These poor transport properties are even more pronounced in the case of **1** with the sulfur anchor group in meta positions. The perpendicular oligophenyleneethynyl (OPE) rod with terminal pyridine anchor groups is the active component of the switch. In an electrochemically controlled junction, the coordination of the pyridine nitrogen should depend on the surface potential of both electrodes with respect to a reference electrode ($U_{\text{Ref.}}$ in Figure 1).

At a negative electrode potential, both pyridine groups are not coordinated to the electrode surface due to the electrostatic repulsion between the electrode and the nitrogen lone pair (**1′**-(OFF-state) in Figure 1). The only connection between both electrodes is the OPV backbone with poor electronic transport properties due to its sulfur anchor groups in the meta position. Upon moving $U_{\text{Ref.}}$ into a positive potential regime, the pyridine nitrogens coordinate to the electrode surface. The strong coupling of the OPE rod's π-system via the pyridine nitrogens to both electrodes is expected to provide an efficient transport channel between both electrodes (**1′**(ON-state) in Figure 1). Thus, both states displayed in Figure 1 are expected to differ considerably in their current transport properties. Furthermore, the switching process is expected to be fully reversible, as the potential dependent surface coordination will be reversible and the active molecule has to remain in the junction, as it is immobilized by the sulfur-terminated less-conducting rod.

Results and Discussion

Synthesis and Characterization. Both target structures **1** and **2** consist of a terminally acetylsulfanyl functionalized OPV rod and a terminally pyridine functionalized OPE rod with a common central benzene unit. The synthetic strategy is to assemble the OPV rod in first place by Wittig-type chemistry.[43] Subsequently, the transversal OPE rod will be assembled by Sonogashira−Hagihara coupling reactions.[44,45] In addition to the functional groups required for the Wittig reaction (aldehyde and triphenylphosphonium salt), a suitably functionalized building block for the cruciforms central phenyl ring comprises already leaving groups allowing the further assembly of the transversal rod, while an ideal building block of the terminal phenyl rings of the OPV rod comprises already the sulfur anchor group. The syntheses of the required functionalized building blocks are displayed in Scheme 1.

Commercially available *p*-xylene (**5**) was iodinated to 2,5-diiodo-*p*-xylene (**6**).[46] The bromination of both methyl groups of **6** turned out to be challenging in spite of several reported procedures.[47,48] Double bromination of one methyl group is often observed and besides the desired product **7**, considerable amounts of compound **8** arising from a halogen exchange reaction were provided at any condition. However, both reaction products **7** and **8** can be separated by crystallization and derivative **8** is of particular interest as it enables the controlled assembly of asymmetric OPE rods due to the substantial difference in reactivity of both halogens in metal-catalyzed cross-coupling reactions. However, treating **7** with triphenylphosphine provided the desired Wittig salt **9** in quantitative yield. The benzaldehydes **14** and **15**, comprising a *tert*-butylsulfanyl group in the meta and para position, respectively, as a second precursor of the Wittig reaction, have been synthesized from the corresponding fluorine derivatives **10** and

(43) Maryanoff, B. E.; Reitz, A. B. *Chem. Rev.* (*Washington, DC, U.S.*) **1989**, *89*, 863−927.
(44) Sonogashira, K.; Tohda, Y.; Hagihara, N. *Tetrahedron Lett.* **1975**, 4467−4470.
(45) de Meijere, A.; Diederich, F., Eds. *Metal-Catalyzed Cross-Coupling Reactions*, 2nd completely revised and enlarged edition; Wiley-VCH: Weinheim, Germany, 2004; Vol. 2.
(46) Wirth, H. O.; Herrmann, F. U.; Kern, W. *Makromol. Chem.* **1964**, *80*, 120−140.
(47) Wilson, J. N.; Windscheif, P. M.; Evans, U.; Myrick, M. L.; Bunz, U. H. F. *Macromolecules* **2002**, *35*, 8681−8683.
(48) Wheland, R. C.; Martin, E. L. *J. Org. Chem.* **1975**, *40*, 3101−3109.

SCHEME 1. Synthesis of the Functionalized Building Blocks 9, 14, 15 and 18[a]

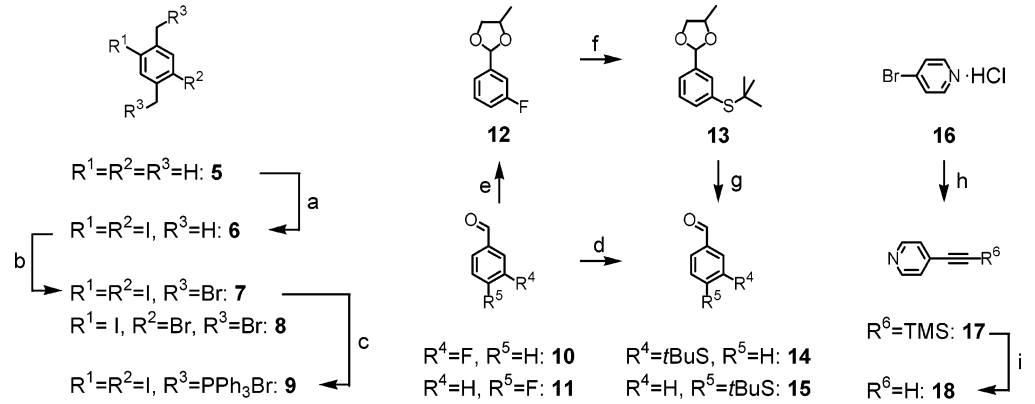

[a] Reagents and conditions: (a) I_2, HIO_3, glacial CH_3COOH, concd H_2SO_4, $CHCl_3$, H_2O, 85 °C, 4 h, 79%. (b) Br_2, $BrCH_2CH_2Br$, 135 °C, 6 h, 20%. (c) PPh_3, DMF, 85 °C, 100%. (d) **11** → **15**: NaS^{t}Bu, DMI, rt, 20 h, 74%. (e) $HOCH_2CHOHCH_3$, pTSOH, toluene, 98 °C, o/n, 84%. (f) NaS^{t}Bu, DMI, 150 °C, o/n, 66%. (g) 0.5 M HCl, dioxane, rt, 1 h, 92%.(h) Trimethylsilylacetylene , $Pd(PPh_3)_4$, CuI, THF, i-Pr_2NH, 2.5 h, rt, 70%. (i) TBAF, THF, 0 °C→rt, 1 h, 83%.

SCHEME 2. Synthesis of the Cruciforms 1−4[a]

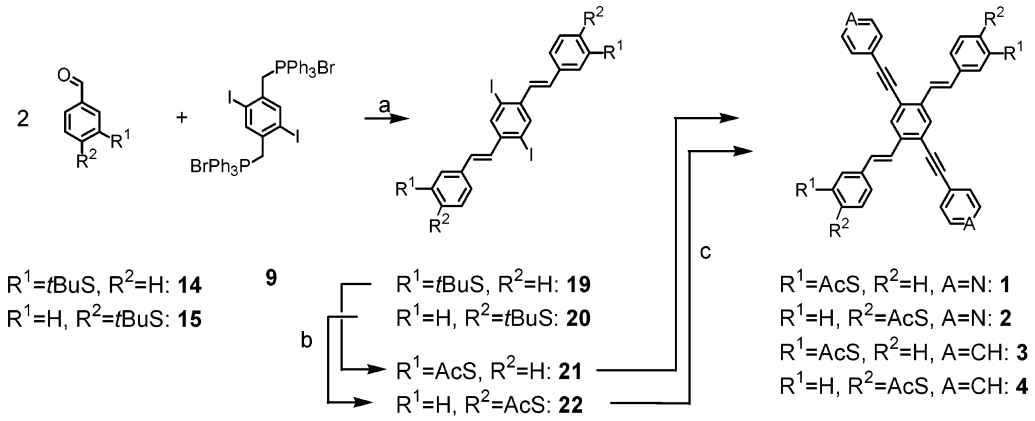

[a] Reagents and conditions: (a) 50% aq NaOH, CH_2Cl_2, rt, 2 d, 70% (**19**), 73% (**20**); (b) BBr_3, CH_3COCl, toluene, rt, (**21**: 2 h, 87%), (**22**: 2.5 h, 80%). (c) **1**: **18**, $Pd(PPh_3)_4$, CuI, THF, i-Pr_2NH, 24 h, 45 °C, 51%. **2**: **18**, $Pd(PPh_3)_4$, CuI, THF, i-Pr_2NH, 22 h, 50 °C, 52%. **3**: Ethynylbenzene, $Pd(PPh_3)_4$, CuI, THF, i-Pr_2NH, 3.5 h, 40 °C, 53%. **4**: Ethynylbenzene, $Pd(PPh_3)_4$, CuI, THF, i-Pr_2NH, 3 h, rt, 43%.

11. With sodium *tert*-butylthiolate as the nucleophile, the protected sulfur anchor group was introduced in a S_NAr reaction. It was chosen to introduce the sulfur as *tert*-butyl thioether for two reasons, namely its robustness in the harsh basic conditions of the Wittig reaction and its efficient transprotection to the desired acetylsulfanyl group.[49,50] The substantially increased reactivity of aromatic systems with an electron withdrawing substituent in the ortho or para position with respect to the leaving group in S_NAr reactions[51] is nicely reflected by both commercially available precursors **10** and **11**. While compound **11**, with the electron withdrawing aldehyde in the para position to the fluorine substituent, reacts with sodium *tert*-butylthiolate to the functionalized aldehyde **15** at room temperature, the substitution of the fluorine atom of **10** requires a considerably elevated reaction temperature. To eliminate side reactions under these harsher reaction conditions, the aldehyde function of **10** was first protected as acetal **12**. After introduction of the sulfur, the functionalized acetal **13** is deprotected to the desired aldehyde **14**. The assembly of 4-ethynylpyridine as the required building block is based on a Sonogashira−Hagihara coupling reaction and **18** was obtained as a photosensitive colorless solid in two steps.[52,53]

With all required building blocks **9**, **14**, **15**, and **18** in hand, the cruciform structures were assembled as displayed in Scheme 2. In a two-phase Wittig reaction, the aldehyde (**14** or **15**) and the bis-phosphonium salt **9** in methylene chloride (CH_2Cl_2) were vigorously stirred with an equal volume of a 50% aqueous sodium hydroxide (NaOH) solution. After workup, an isomeric mixture of all possible isomers (EE, EZ, ZZ) was isolated in 83% yield. The mixture was then refluxed in toluene with traces of iodine to increase the fraction of the thermodynamically most stable EE-isomer by an iodine addition−elimination reaction sequence. Subsequent recrystallization provided both desired EE-isomers **19** and **20** as yellow solids in yields of 70% and 73%, respectively.

As acetyl protected thiophenols tolerate the mild basic conditions of Sonogashira−Hagihara coupling reactions the

(49) Błaszczyk, A.; Elbing, M.; Mayor, M. *Org. Biomol. Chem.* **2004**, *2*, 2722−2724.
(50) Stuhr-Hansen, N. *Synth. Commun.* **2003**, *33*, 641−646.
(51) Brückner, R., Ed. *Reaction Mechanisms in Organic Chemistry*; Spektrum Akademischer Verlag: Berlin, Germany, 1996.
(52) Ziessel, R.; Suffert, J.; Youinou, M.-T. *J. Org. Chem.* **1996**, *61*, 6535−6546.
(53) Stang, P. J.; Whiteford, J. A.; Lu, C. V.; Stang, P. J. *J. Am. Chem. Soc.* **1997**, *119*, 2524−2533.

SCHEME 3. Different Strategies for the Assembly of the OPE Subunit of the Cruciform 1[a]

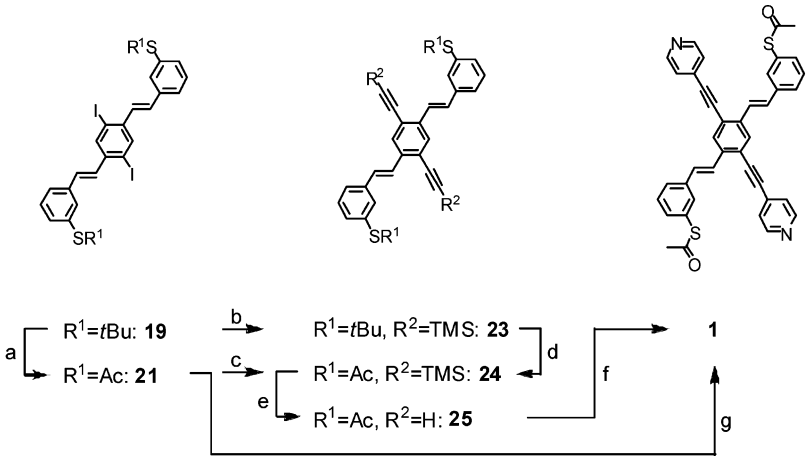

[a] Reagents and conditions: (a) BBr_3, CH_3COCl, toluene, rt, 2h, 87%. (b) Trimethylsilylacetylene, $Pd(PPh_3)_4$, CuI, THF, i-Pr_2NH, 2.5 h, rt, 80%. (c) Trimethylsilylacetylene, $Pd(PPh_3)_4$, CuI, THF, i-Pr_2NH, 2 h, 60 °C, 80%. (d) BBr_3, toluene, AcCl, 2h, rt, 11%. (e) TBAF, AcOAc, AcOH, THF, 40 min, 0 °C→rt, 80%. (f) 4-Iodopyridine, $Pd(PPh_3)_4$, CuI, THF, i-Pr_2NH, 5 h, rt, 50%. (g) **18**, $Pd(PPh_3)_4$, CuI, THF, i-Pr_2NH, 24 h, 45 °C, 51%.

SCHEME 4. The Cruciform 2 and Its Intrinsic Molecular Rod Fragments 27 and 28, Together with the Cruciform 4 Lacking the Pyridine Nitrogens as Potential Anchor Groups at the End of the OPE Rod

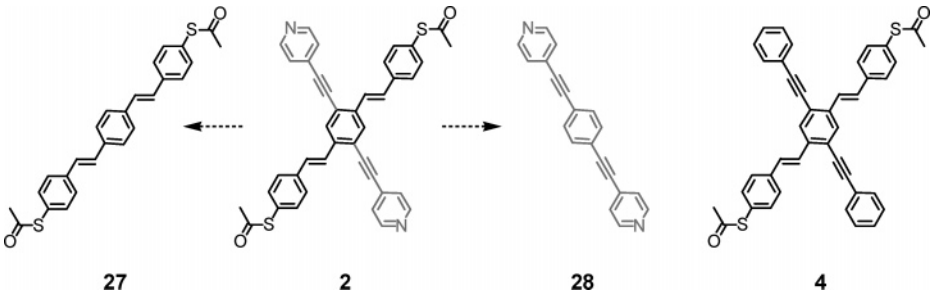

strategy is to transprotect the sulfur of the functionalized OPV-rods prior to the assembly of its transversal OPE-rods. For the transprotection of *tert*-butylsulfanyl groups to acetylsulfanyl groups two alternative protocols have been reported.[49,50] The rather poor solubility of both starting materials **19** and **20** favored the protocol based on Lewis acids[50] instead of catalytic amounts of bromine[49] as reagent to cleave the *tert*-butyl group. The two acetylated compounds **21** and **22** were obtained in 87% and 80% yields, respectively.

To assemble the perpendicular OPE rod of the cruciform structures several alternative synthetic strategies have been considered and for target structure **1** the potential of the different synthetic routes has been investigated to some extent as displayed in Scheme 3.

Transprotection of the sulfur after functionalization of **19** with TMS-acetylene turned out to be troublesome and disqualified the route over intermediate **23** (b and d in Scheme 3). In the case of intermediate **24**, TBAF as reagent to remove the TMS protection groups of the acetylene also attacks the acetyl protection group of the terminal thiophenols. However, a protocol based on in situ reprotection of thiophenols was applied successfully and provided **25** in 80% yield.[42] Coupling of 4-iodopyridine to **25** provided the desired cruciform target structure **1** in 50% yield. Alternatively, Sonogashira−Hagihara coupling of **21** and **18** results in the desired cruciform structure **1** as well. It is noteworthy that this strategy has been reported by Bunz and co-workers recently for the assembly of OPV/OPE cruciform structures.[34,36] With a comparable overall yield but considerable increase of the relative yield (51% for step g compared to 32% for steps c, e, and f in Scheme 3) only considering the elaborate precursor **21**, the parallel assembly (steps a and g in Scheme 3) was favored compared with the sequential assembly (steps a, c, e, and f in Scheme 3). Thus, similar reaction sequences have been applied for the assembly of the cruciform **2** with the acetyl sulfanyl groups in the para position and also for the two cruciform derivatives **3** and **4** lacking the pyridine nitrogen, which are intended as control compounds enabling the investigation of the switching mechanism in detail (synthesis given in the Supporting Information). Starting from the acetyl protected diiododerivatives **21** and **22**, the cruciforms **2**, **3**, and **4** were obtained in yields of 52%, 53%, and 43%, respectively. In addition, the two substructures of compound **2** namely the OPV molecular rod **27** with terminal sulfur anchor groups in the para position and the OPE molecular rod **28** with two terminal pyridine units[54] were synthesized to trace the origin of the observed transport behavior in control experiments with the parent structural motives (Scheme 4).

All new compounds were fully characterized by conventional analytical and spectroscopic techniques like ^1H and ^{13}C NMR spectroscopy and mass spectrometry. Due to solubility problems, no ^{13}C spectra were obtained for compounds **7**, **9**, and **22**. Furthermore, the purity of the compounds has been investigated either by elemental analysis or by HPLC. It is noteworthy that in spite of impurity-free NMR spectra and HPLC protocols, all

(54) Grummt, U. W.; Birckner, E.; Klemm, E.; Egbe, D. A. M.; Heise, B. *J. Phys. Org. Chem.* **2000**, *13*, 112−126.

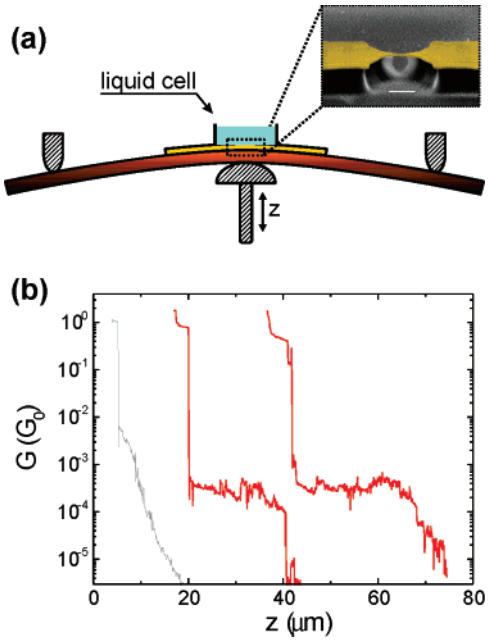

FIGURE 2. (a) Schematics of the MCBJ setup. The sample is inserted in a three-point bending mechanism allowing the controlled elongation of the lithographically patterned Au bridge. Inset: SEM image of the free-standing Au bridge. Scale bar: 500 nm. (b) Typical conductance vs elongation curves for the solvent (gray) and compound **27** (red). Clear conductance plateaus develop when a molecule is trapped within the junction. The solvent was a 0.17 mM TBAOH solution in THF/mesitylene (1/4)

reported cruciform structures **1**−**4** displayed slightly too low carbon signals in their elemental analysis.

Integration and Transport Investigations. Due to their structural complexity and spatial extension, it is a priori unclear whether the cruciform structures **1**−**4** can be efficiently contacted for subsequent transport characterization. Before attempting any switching of these compounds, their immobilization on a single molecule level between contact electrodes has to be demonstrated. For this purpose, a mechanically controllable break junction (MCBJ) setup operated in a liquid environment has been developed recently.[55] The liquid environment will subsequently allow the extension of the setup to gain electrochemical control over the surface potential of both electrodes.

The setup is schematically represented in Figure 2a. A sample consists of a lithographically fabricated gold structure with a freely suspended 80 to 150 nm wide constriction in the central part (inset). The substrate is a flexible spring steel foil with a several micrometers thick polyimide isolation layer. When mounted in a three-point bending mechanism, the suspended Au wire can be elongated in a controlled manner and, ultimately, broken. When broken in the presence of molecules with anchoring groups, the two tips of the broken wire form ideal electrodes to contact single molecules. A flexible viton tube mounted on a spring-loaded support serves as the liquid cell to deliver the molecules in situ.

During the breaking process, the conductance of the junction is monitored via a homemade current−voltage converter. To immobilize molecules in the junction, the cell (cell volume: 3 mL) was flooded with a 0.25 mM solution of the molecule under

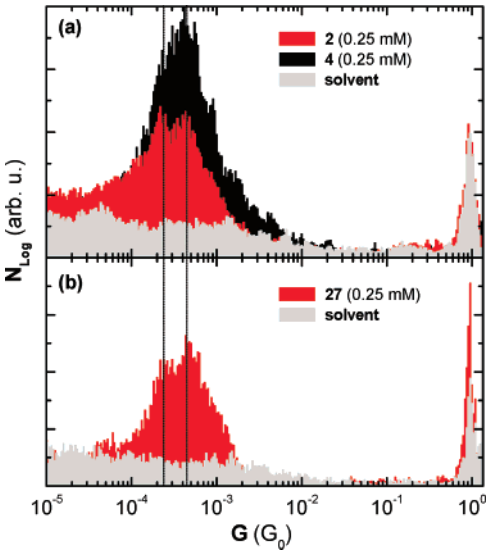

FIGURE 3. (a) Conductance histogram for the pure solvent (gray), **2** (red), and **4** (black). The histograms are made out of 200 consecutive conductance curves. (b) Characterization of OPV (**27**) (red) as a reference compound. The histogram is made of 100 consecutive conductance curves. All histograms were normalized to allow a proper comparison. The solvent was a 0.17 mM TBAOH solution in THF/mesitylene (1/4).

investigation in a degassed THF/mesitylene mixture (1/4). The acetyl protection groups of the thiophenol anchor groups were removed in situ by adding 50 μL of a 10 mM solution of tetrabutylammonium hydroxide (TBAOH) in THF. Hereafter, the term solvent will refer to the degassed THF/mesitylene mixture (1/4) with the deprotection agent. Typical conductance vs elongation curves during junction opening are shown in Figure 2b for the solvent (gray) and compound **27** (red) as a 0.25 mM solution in the solvent mixture.

After a plateau close to $1G_0$ due to the breaking of a final monatomic Au contact, the conductance drops abruptly, signaling the opening of a gap in the Au bridge. In the presence of **27** in the liquid cell, conductance plateaus develop in the region $10^{-3}G_0$ to $10^{-4}G_0$, indicating the trapping of molecules within the junction. By repeatedly opening and closing the gap, we can obtain good statistics for the molecular junction formation. For this work, about 200 consecutive open−close cycles for each solution were recorded. Note that, during the measurements, the liquid cell was kept under argon atmosphere to suppress any oxygen-promoted oxidation process like disulfide formation.

From all individual measurements obtained for the solvent or a specific compound, conductance histograms have been made (Figure 3). Plateaus in the individual curves translate as peaks in the histograms, denoting the most favorable microscopic conformation for the molecular junction. This analysis was done accordingly to González and co-workers.[56] The peak in the conductance histogram is interpreted as the typical signature of a particular molecule.[56]

No molecular signature could be detected for cruciform **1**. Even though OPE rod-type structures with sulfur anchor groups in the meta position have been investigated in a MCBJ setup in vacuum,[42] similar lock-in characteristics of the OPV backbone

(55) Grüter, L.; González, M. T.; Huber, R.; Calame, M.; Schönenberger, C. *Small* **2005**, *1*, 1067−1070.

(56) González, M. T.; Wu, S.; Huber, R.; van der Molen, S. J.; Schönenberger, C.; Calame, M. *Nano Lett.* **2006**, *6*, 2238−2242.

bearing sulfur anchor groups in the meta position were not observed in the liquid environment. We foresee that the subunit investigated displayed a conductance below our detection threshold ($\sim 10^{-6} G_0$). To improve the transport properties of the OPV rod, cruciform **2** with sulfur anchor groups in the para position was designed and synthesized.

All three molecules comprising the para-thiolated OPV backbone (**2**, **4**, and **27**) have been integrated successfully in the MCBJ setup in the liquid environment and their conductance histograms are displayed in Figure 3, together with the conductance histogram of the solvent solely containing the deprotection agent (TBAOH). Besides the peak at $G_0 = 2e^2/h$ which corresponds to the breaking of the Au bridge, the measurement of the solvent (gray in Figure 3a) does not show any peaks. In contrast to that, both cruciforms **2** (red in Figure 3a) and **4** (black in Figure 3a) display a clear molecular signature in the tunnel region ($G \ll G_0$) of the conductance histogram.

We assign this signature to the OPV substructure of these cruciforms, immobilized with their terminal sulfur groups in the para position and forming a covalent S−Au bond. As a control experiment, the OPV rod **27** was inspected in the junction under the same conditions (red in Figure 3b). The similarity between the recorded histograms for **2** and **27** is quite striking. Both display two marked peaks at $(2.2 \times 10^{-4})G_0$ and $(4.4 \times 10^{-4})G_0$ (vertical dashed lines), which are attributed to one and two molecules in parallel immobilized in the junction.[56] The histogram recorded with cruciform **4** shows also a clear molecular signature in the same conductance regime, with the first two peaks being more blurred, although a shoulder at $(2.2 \times 10^{-4})G_0$ is still perceivable. As additional control experiment, an OPE rod **28** comprising terminal pyridine groups as the second rod-like subunit of cruciform **2**, has been investigated under the same conditions in the MCBJ. No molecular signature has been observed in this conductance regime, further corroborating that the OPV subunit of the cruciform is the trapped structure. These preliminary investigations demonstrate that designed molecular structures encompassing significant complexity can be successively immobilized in a MCBJ setup in a liquid environment. This confirms the pertinence of developing molecular complexes with added functionality such as that proposed with these cruciforms. We additionally demonstrate that the molecules were anchored via the thiol end groups with the OPV subunit as the immobilized rod.

Conclusion

A new switching concept based on the electrochemically triggered reversible coordination between a single molecule and the surfaces of electrodes is suggested. New cruciform structures consisting of terminally pyridine functionalized OPE rods for the reversible coordination on the metal electrodes and transversal OPV rods comprising terminal sulfur anchor groups to hold the molecule in the junction have been synthesized and fully characterized as model compounds to investigate the proposed switching mechanism. Furthermore, first immobilization attempts of these cruciforms in a mechanically controlled break junction in a liquid environment are presented. The observed histograms corroborate not only the sulfur-terminated OPV rod as the bridging structure between both electrodes, but also that molecules comprising additional functional properties can be immobilized on a single molecule level in the MCBJ setup. Currently, we are assembling an MCBJ experiment comprising the required reference electrode to control the surface potentials of both electrodes to be able to investigate the switching potential of these molecular junctions and we are synthesizing the next generation of cruciform structures for which a considerably increased difference between both states is hypothesized.

Experimental Section

2-(3-Fluorophenyl)-4-methyl-1,3-dioxolane (12). 3-Fluorobenzaldehyde (2.00 mL, 19.0 mmol, 1.0 equiv) was dissolved in 30 mL of toluene. Molecular sieves (3 Å) and *p*-toluenesulfonic acid (1.70 g, 9 mmol, 50 mol %) were added. The resulting mixture was stirred over night at 100 °C. The reaction mixture was then filtrated over 1 cm of silica gel, washed with CH_2Cl_2, and evaporated. The product was purified by column chromatography (CC) (silica gel, 3 × 5 cm, CH_2Cl_2) to yield a colorless liquid (2.73 g, 15.0 mmol, 79%). TLC R_f 0.51 (CH_2Cl_2/hexane, 1:1); ^{1}H NMR (250 MHz, $CDCl_3$, δ/ppm) 7.39−7.16 (3H, m), 7.05 (1H, m), 5.95−5.80 (1H, 2s), 4.42−4.31 (1H, m), 4.27−4.10 (1H, m), 3.62−3.53 (1H, m), 1.41−1.34 (3H); ^{13}C NMR (101 MHz, $CDCl_3$, δ/ppm) 164.4, 162.0, 141.7, 141.0, 130.4, 130.3, 122.7, 122.4, 116.4, 116.2, 113.8, 113.5, 103.5, 102.6, 74.1, 72.9, 72.4, 18.9, 18.7; MS (FAB) 181 (100%, M^+), 137 (24%), 123 (94%); EA calcd: C 65.92, H 6.09, found: C = 65.59, H = 6.16; IR (neat, ν, cm^{-1}) 2977.9, 2877.6, 1593.1, 1454.2, 1091.6.

2-(3-(*tert*-Butylthio)phenyl)-4-methyl-1,3-dioxolane (13). 2-(3-Fluorophenyl)-4-methyl-1,3-dioxolane (**12**) (11.22 g, 61.6 mmol, 1.0 equiv) was dissolved in 120 mL of DMI. Sodium 2-methyl-2-propanethiolate (13.8 g, 123.2 mmol, 2.0 equiv) was added and the reaction was stirred overnight at 150 °C. The reaction mixture was extracted with water and toluene. The organic phase was washed with water. The aqueous phase was washed three times with toluene. The combined organic phases were dried over Na_2SO_4 and evaporated. The crude was purified by CC (silica gel, 5 × 12 cm, toluene/CH_2Cl_2, 3:2) to give **13** as a colorless liquid (10.24 g, 40.6 mmol, 66%). TLC R_f 0.45 (toluene/CH_2Cl_2, 3:2); ^{1}H NMR (250 MHz, $CDCl_3$, δ/ppm) 7.68−7.19 (4H, m), 5.99−5.84 (1H, 2s), 4.46−4.13 (2H, m), 3.67−3.57 (1H, m), 1.40−1.35 (3H, m), 1.32 (9H, s); ^{13}C NMR (101 MHz, $CDCl_3$, δ/ppm) 139.5, 138.8, 138.4, 133.2, 128.9, 127.4, 127.2, 104.1, 103.1, 74.0, 72.8, 72.4, 71.8, 46.4, 31.4, 19.0, 18.8; MS (EI) 252 (32%, M^+), 196 (100%), 163 (7%), 137 (30%); EA calcd: C = 66.63, H = 7.99, found: C = 66.66, H = 7.94; IR (neat, ν, cm^{-1}) 2939.3, 2862.2, 1685.7, 1504.3, 1442.7, 1396.37.

1,4-Bis(bromidetriphenylphosphinemethyl)-2,5-diiodobenzene (9). 1,4-Bis(bromomethyl)-2,5-diiodobenzene (1.960 g, 3.82 mmol, 1.0 equiv) was dissolved in 36 mL of dry DMF at 85 °C. PPH_3 (2.002 g, 7.64 mmol, 2.0 equiv) was added. The homogeneous solution was stirred at 85 °C. After 5 min a white precipitate was formed. The reaction mixture was cooled to room temperature. The precipitate was filtered off, washed with toluene, and dried under high vacuum to give **9** as a white powder (3.97 g, 3.82 mmol, 100%). ^{1}H NMR (250 MHz, $CDCl_3$, δ/ppm) 7.69 (32H, m), 5.70 (4H, sb); MS (FAB) 440 (38%, M^{2+}), 307 (15%), 262 (100%); mp 276−277 °C; IR (neat, ν, cm^{-1}) 2823.6, 1666.4, 1434.9, 1099.4.

1,4-Bis(3-thio-*tert*-butylstyryl)-2,5-diiodobenzene (19). 14 (1.68 g, 8.65 mmol, 3.0 equiv) was dissolved in 150 mL of CH_2Cl_2. The phosphonium salt **9** (3.00 g, 2.88 mmol, 1.0 equiv) was added, then 100 mL of aq 50% NaOH was added and the solution was stirred for 2.5 days at room temperature. The reaction mixture was then extracted. The aqueous phase was washed twice with dichloromethane. The combined organic phases were dried over Na_2SO_4, filtrated, and evaporated. The crude was chromatographed (silica gel, 3 × 12 cm, CH_2Cl_2) to give an isomeric mixture in 83% yield. The isomers were refluxed in toluene containing iodine in catalytic amount overnight. The EE-product was precipitated, then it was filtrated off and washed with hexane to give a yellow solid (1.43 g, 2.01 mmol, 70%). TLC R_f 0.30 (hexane:ethyl acetate 20:1); ^{1}H

NMR (250 MHz, $CDCl_3$, δ/ppm) 8.12 (2H, s), 7.74 (2H, s), 7.60 (2H, d, $^3J_{HH}$ = 7.70 Hz), 7.51 (2H, d, $^3J_{HH}$ = 7.70 Hz), 7.39 (2H, t, $^3J_{HH}$ = 7.70 Hz), 7.25 (2H, d, $^3J_{HH}$ = 16.06 Hz), 7.00 (2H, d, $^3J_{HH}$ = 15.73 Hz), 1.36 (18H, s); ^{13}C NMR (101 MHz, $CDCl_3$, δ/ppm) 141.2, 137.6, 137.4, 136.8, 136.4, 133.8, 132.2, 131.5, 129.3, 127.4, 100.7, 46.5, 31.4; MS (EI) 710 (15%, M^+), 653 (11%), 598 (46%), 551 (12%), 469 (5%); EA calcd: C = 50.71, H = 4.54, found: C = 50.24, H = 4.46; mp 247−248 °C; IR (neat, ν, cm^{-1}) 3055.0, 2958.6, 2858.3, 1809.1, 1566.1, 1454.2.

1,4-Bis(4-thio-*tert*-butylstyryl)-2,5-diiodobenzene (20). 15 (190 mg, 0.98 mmol, 3.0 equiv) and the phosphonium salt (**9**) (340 mg, 0.33 mmol, 1.0 equiv) were dissolved in 7 mL of CH_2Cl_2, then 6 mL of 50% aq NaOH was added and the solution was stirred vigorously for 69 h. The reaction mixture was then extracted with water/toluene. The combined organic phases were dried over Na_2SO_4, filtrated, evaporated, and chromatographed (silica gel, 2 × 12 cm, CH_2Cl_2). The isomeric mixture was then refluxed in toluene with catalytic amounts of iodine overnight. It was then extracted with 10% aq $NaHSO_3$, washed with water, dried over Na_2SO_4, evaporated, and recrystallized from toluene to obtain **20** as a yellow solid (170 mg, 0.24 mmol, 73%). TLC R_f 0.74 (CH_2Cl_2); ^{1}H NMR (250 MHz, $CDCl_3$, δ/ppm) 8.08 (2H, s), 7.53 (8H, m), 7.24 (2H, d, $^3J_{HH}$ = 16.06 Hz), 6.98 (2H, d, $^3J_{HH}$ = 16.06 Hz), 1.32 (18H, s); ^{13}C NMR (101 MHz, $CDCl_3$, δ/ppm) 141.1, 138.2, 137.2, 136.8, 133.5, 132.1, 131.7, 127.3, 100.8, 46.8, 31.4; MS (EI) 710.0 (42.3%, M^+), 597.8 (100%); EA calcd: C = 50.71, H = 4.54, found: C = 50.74, H = 4.55; IR (neat, ν, cm^{-1}) 3018.9, 2954.7, 2858.3, 1892.5, 1356.3; mp 232−233 °C.

1,4-Bis(3-thioacetylstyryl)-2,5-diiodobenzene (21). 1,4-Bis(3-thio-*tert*-butylstyryl)-2,5-diiodobenzene (**19**) (2.13 g, 3.00 mmol, 1.0 equiv) was dissolved in a degassed mixture of 500 mL of dry toluene and 100 mL of acetyl chloride, then 6 mL of a 1 M solution of BBr_3 in CH_2Cl_2 (1.408 mol, 2.0 equiv) was added. The reaction was stirred for 1 h at room temperature. Another 4.5 mL of the 1 M solution of BBr_3 in CH_2Cl_2 was added and then the mixture was stirred for another hour at room temperature. While cooling with an ice-bath, the reaction mixture was quenched with water. The product precipitated as a yellow solid, which was filtrated off and washed with water. The organic phase was washed with water, evaporated, and recrystallized from toluene to give more of product **21** (1.75 g, 2.56 mmol, 87%). TLC R_f 0.43 (CH_2Cl_2); ^{1}H NMR (250 MHz, $CDCl_3$, δ/ppm) 8.06 (2H, s), 7.59 (2H, d, $^3J_{HH}$ = 7.58 Hz), 7.58 (2H, d, $^4J_{HH}$ = 1.52 Hz), 7.44 (2H, t, $^3J_{HH}$ = 7.58 Hz), 7.35 (2H, d, $^3J_{HH}$ = 7.58 Hz), 7.19 (2H, d, $^3J_{HH}$ = 15.66 Hz), 6.96 (2H, d, $^3J_{HH}$ = 16.17 Hz), 2.46 (6H, s); ^{13}C NMR (101 MHz, $CDCl_3$, δ/ppm) 194.2, 141.2, 138.1, 136.9, 134.6, 133.3, 131.9, 131.8, 130.0, 129.1, 128.2, 100.7, 30.7; MS (EI) 681 (84%, M^+), 639 (34%), 597 (49%); EA calcd: C = 45.76, H = 2.95, found: C = 46.20, H = 2.95; mp 214−215 °C; IR (neat, ν, cm^{-1}) 3051.1, 2958.6, 1890.1, 1697.2, 1118.6.

1,4-Bis(4-thioacetylstyryl)-2,5-diiodobenzene (22). 20 (356 mg, 0.521 mmol, 1.0 equiv) was dissolved in a degassed mixture of 85 mL of dry toluene and 15 mL of concentrated AcCl. BBr_3 (1 M in CH_2Cl_2, 3.6 mL, 3.6 mmol, 6.9 equiv) was added portionwise during 2.5 h at room temperature. The reaction mixture was quenched with water at 0 °C. A precipitate was formed, which was filtered off and recrystallized from toluene to give **15** as a yellow solid (283 mg, 0.41 mmol, 80%). TLC R_f 0.48 (CH_2Cl_2); ^{1}H NMR (250 MHz, $CDCl_3$, δ/ppm) 8.08 (2H, s), 7.59 (4H, d, $^3J_{HH}$ = 8.37 Hz), 7.43 (4H, d, $^3J_{HH}$ = 8.37 Hz), 7.24 (2H, d, $^3J_{HH}$ = 16.06 Hz), 6.97 (2H, d, $^3J_{HH}$ = 16.16.40 Hz), 2.45 (6H, s); MS (EI) 681.8 (76%, M^+), 639.8 (56%), 597.8 (100%); EA calcd: C = 45.76, H = 2.95, found: C = 45.81, H = 2.97; mp 253−255 °C; IR (neat, ν, cm^{-1}) 2920.0, 2854.5, 1905.5, 1689.5, 1122.5.

1,4-Bis(3-thioacetylstyryl)-2,5-bis(ethynyl-4-pyridine)benzene (1). 4-(Ethynyl)pyridine (**18**) (2.2 equiv, 1.65 mmol, 170 mg), 1,4-bis(3-thioacetylstyryl)-2,5-diiodobenzene (**21**) (1.0 equiv, 0.76 mmol, 520 mg), $Pd(PPh_3)_4$ (10 mol %, 87 mg), and CuI (10 mol %, 14 mg) were dissolved in a well-degassed mixture of 90 mL of dry THF and 10 mL of diisopropylamine. The reaction mixture was stirred for 24 h at 45 °C and was then poured into a mixture of 250 mL of hexane and 250 mL of aq 5% NH_4OH. The precipitated solid was collected, dissolved in a minimum amount of CH_2Cl_2, and dropped into 250 mL of rapidly stirring hexane. The precipitate was collected and recrystallized from toluene/CH_2Cl_2 to give **1** as a yellow solid (246 mg, 0.39 mmol, 51%).

1,4-Bis(3-thioacetylstyryl)-2,5-bis(ethynyl)benzene (**24**) (1.0 equiv, 0.167 mmol, 80 mg) was dissolved in a degassed mixture of 15 mL of dry THF and 2.5 mL of diisopropylamine. Then 4-pyridine-halide (2.2 equiv, 0.368 mmol), $Pd(PPH_3)_4$ (10 mol %, 42 mg), and CuI (10 mol %, 7 mg) were added. The reaction mixture was stirred for 24 h at 45 °C (X = Br) or room temperature (X = I), respectively, and was then poured to a mixture of 100 mL of hexane and 100 mL of aq 5% NH_4OH. The precipitated solid was collected, dissolved in a minimum amount of CH_2Cl_2, and dropped into 200 mL of rapidly stirring hexane. The precipitate was collected and recrystallized from toluene/CH_2Cl_2 to give **1** as a yellow solid (X = Br: <10%; X = I: 52 mg, 50%). ^{1}H NMR (250 MHz, $CDCl_3$, δ/ppm) 8.67 (4H, d, $^3J_{HH}$ = 6.06 Hz), 7.92 (2H, s), 7.64 (2H, s), 7.61 (2H, d, $^3J_{HH}$ = 16.67 Hz), 7.58 (2H, d, $^3J_{HH}$ = 8.08 Hz), 7.46 (4H, d, $^3J_{HH}$ = 6.06 Hz), 7.45 (2H, t, $^3J_{HH}$ = 8.08 Hz), 7.35 (2H, $^3J_{HH}$ = 7.58 Hz), 7.26 (2H, d, $^3J_{HH}$ = 16.67 Hz), 2.47 (6H, s); ^{13}C NMR (101 MHz, $CDCl_3$, δ/ppm) 194.4, 150.4, 138.5, 138.1, 134.3, 133.1, 131.3, 131.0, 130.1, 129.8, 129.2, 128.2, 126.5, 125.9, 122.5, 93.7, 92.1, 30.8; MS (MALDI): 632 (M^+); mp 227.7−228.7 °C (melting followed by decomposition); IR (neat, ν, cm^{-1}) 3049.7, 3008.3, 2201.1, 1699.2, 1588.3, 953.7; GPC (oligopore 6 μm, toluene, UV/vis photodiode array detector) area 99.6%.

1,4-Bis(4-thioacetylstyryl)-2,5-bis(ethynyl-4-pyridine)benzene (2). 22 (155 mg, 0.227 mmol, 1.0 equiv) was dissolved in a well-degassed mixture of 20 mL of dry THF and 2.5 mL of diisopropylamine. **18** (58.6 mg, 0.568 mmol, 2.5 equiv), $Pd(PPh_3)_4$ (20 mg, 0.017mmol, 7.6 mol %), and CuI (8 mg, 0.042 mmol, 18.5 mol %) were added and the solution was stirred 7 h at room temperature and 15 h at 50 °C. The reaction mixture was then poured to a mixture of 50 mL of 5% aq NH_4OH and 50 mL of hexane. The precipitate was filtrated off, dissolved in CH_2Cl_2, and precipitated into 60 mL of rapidly stirring hexane. The insoluble material was collected and recrystallized from toluene to give a yellow solid (75 mg, 0.119 mmol, 52%). ^{1}H NMR (250 MHz, $CDCl_3$, δ/ppm) 8.71 (4H, d, $^3J_{HH}$ = 6.36 Hz), 7.97 (2H, s), 7.80 (2H, d, $^3J_{HH}$ = 16.40 Hz), 7.63 (4H, d, $^3J_{HH}$ = 8.34 Hz), 7.48 (4H, d, $^3J_{HH}$ = 6.02 Hz), 7.47 (4H, d, $^3J_{HH}$ = 8.03 Hz), 7.31 (2H, d, $^3J_{HH}$ = 16.06 Hz), 2.48 (6H, s); ^{13}C NMR (101 MHz, $CDCl_3$, δ/ppm) 194.3, 150.4, 138.4, 138.4, 138.1, 135.3, 131.3, 131.2, 129.9, 128.2, 127.9, 126.7, 125.8, 122.5, 93.6, 92.0, 30.7; MS (MALDI) 633.6 (100%,M^+); IR (neat, ν, cm^{-1}) 3046.4, 2217.5, 1699.2, 1588.3; mp 192.2−199.5 °C dec; GPC (oligopore 6 μm, toluene, UV/vis photodiode array detector) area 100%.

Acknowledgment. M.T.G. thanks the "Ministerio de Educación y Ciencia" for financial support. This work was supported by the Swiss National Center of Competence in Research "Nanoscale Science" (NCCR), the Swiss National Science Foundation (SNF), and the European Science Foundation EUROCORES program on Self-Organized Nanostructures (SONS).

Supporting Information Available: NMR spectra of compound **1**−**4**, **6**, **7**, **9**, **14**, **15**, and **17**−**28**, GPC spectra of compounds **1**−**4**, and the synthesis of **3**, **4**, **6**, **7**, **14**, **15**, **17**, **18**, and **24**−**28**. This material is available free of charge via the Internet at http://pubs.acs.org.

JO7013998